Journal of the European Ceramic Society 20 (2000) 2315–2324

The perovskite system $La(Mg_{2/3}Nb_{1/3})O_3$ I. Synthesis, formation and characterisation of powders

Supon Ananta, Rik Brydson, Noel W. Thomas *

Department of Materials, University of Leeds, Leeds LS2 9JT, UK

Received 5 July 1999; received in revised form 19 April 2000; accepted 29 April 2000

Abstract

A perovskite-like phase of lanthanum magnesium niobate, $La(Mg_{2/3}Nb_{1/3})O_3$ (LMN) has been synthesised by a mixed oxide synthetic route. Both magnesium oxide and magnesium carbonate hydroxide pentahydrate have been investigated as magnesium precursors, with the formation of the LMN phase investigated as a function of calcination temperature and dwell time by DTA and XRD. Morever, particle size distribution, morphology, phase composition and crystal structure have been determined via laser diffraction, SEM and TEM/EDX, respectively. A combination of X-ray and electron diffraction studies has demonstrated that heterogeneous powders are produced, with the presence of an MgO-rich phase and varying Mg/Nb ratios within the parent phase of LMN. Minor phases have also been identified as $LaNbO_4$, La_3NbO_7, MgO, $Mg_4Nb_2O_9$ and La_2O_3, with their concentrations decreasing with rising calcination temperature. X-ray and electron diffraction data are supportive of monoclinic symmetry in the parent LMN phase.

Keywords: Crystal structure; La(Mg, Nb)O_3; Perovskites; Phase development; Powders-solid state reaction

1. Introduction

$A(B'B'')O_3$-perovskite-type compounds have been investigated extensively, both from academic and commercial viewpoints. For example, compositions such as $A(B'_{1/3}B''_{2/3})O_3$ [e.g. $Pb(Mg_{1/3}Nb_{2/3})O_3$ (PMN); $Ba(Mg_{1/3}Nb_{2/3})O_3$ (BMN)], $A(B'_{1/2}B''_{1/2})O_3$ [e.g. $Pb(Fe_{1/2}Nb_{1/2})O_3$ (PFN); $La(Mg_{1/2}Ti_{1/2})O_3$ (LMT)), and $A(B'_{2/3}B''_{1/3})O_3$ (e.g. $Pb(Fe_{2/3}W_{1/3})O_3$ (PFW); $La(Zn_{2/3}Nb_{1/3})O_3$ (LZN)] have been synthesised and examined.[1–6] Most of these compounds are probably best known for their dielectric, ferroelectric, ferromagnetic and piezoelectric properties.[1–3] Since these physical properties are strongly dependent on cation ordering phenomena, a recurrent theme has been the dependence of ordering on cationic radii and charges.[7–17]

In recent years, correlations between the dielectric/piezoelectric properties and the ordering behaviour of some complex perovskite systems have been found, e.g. in La-modified PMN (PLMN), La-modified PMN-$PbTiO_3$ (PLMNT) and La-modified $Pb(Zr_xTi_{1-x})O_3$ (PLZT), along with other well established systems.[7–13] Since the most versatile mixed oxide synthetic route to PLMN involves the intermediates PMN and LMN, it is appropriate to focus on the latter compound, i.e. lanthanum magnesium niobate (LMN), of composition $La(Mg_{2/3}Nb_{1/3})O_3$.[18–20]

Very little is known about LMN, since no work has been dedicated to the synthesis of this compound. Moreover, in the current JCPDS database, there is no record of LMN, although some PLMN compounds are included. Furthermore, it has recently been shown that dielectric properties and crystal structure of the PLMN system are very sensitive to the La concentration.[7,18,19]

Recent work on La-modified PMN,[9,18,19] La-modified PMN-PT,[10,13] and the BMN-LMN system[20] has provided some valuable information about LMN. The fabrication of LMN powder using a conventional mixed oxide route with MgO as a magnesium source has also been reported by Lin and Wu[9] in their study of La-modified PMN. In their work, a complex perovskite-type structure with a rhombohedral unit cell ($a = 7.928$ Å;

* Corresponding author at present address: WBB Technology Ltd., Watts Blake Bearne & Co plc, Park House, Courtenay Park, Newton Abbot TQ12 4PS, UK. Tel.: +44-1626-322351; fax: +44-1626-322386.

E-mail address: nthomas@wbb.co.uk (N.W. Thomas).

0955-2219/00/$ - see front matter
PII: S0955-2219(00)00141-2

$\alpha = 89.7^\circ$ space group $R\bar{3}$), was proposed for LMN at room temperature.

The purpose of the present article is to study the phase formation characteristics and processing-structure-property relationships in the compound LMN, with a view to enhancing overall understanding. The study also forms a possible basis for a systematic survey of LMN.

2. Method

2.1. Sample preparation

$La(Mg_{2/3}Nb_{1/3})O_3$ was synthesised by the solid state reaction of appropriate amounts of reagent grade lanthanum oxide, La_2O_3 (Aldrich, >99% purity), niobium oxide, Nb_2O_5 [Alfa (Johnson Matthey), 99.9+% purity] and magnesium oxide; MgO (Aldrich, 99% purity). In order to improve the reactivity of the MgO starting precursor, an alternative route employing magnesium carbonate hydroxide pentahydrate, $(MgCO_3)_4.Mg(OH)_2.5H_2O$ (Aldrich, 99% purity) was also investigated. The following reaction sequences are proposed for the formation of LMN:

1. The conventional mixed oxide route

$$3La_2O_3 + 4MgO + Nb_2O_5 \Rightarrow 6La(Mg_{2/3}Nb_{1/3})O_3 \quad (1)$$

2. The alternative mixed oxide route

$$15La_2O_3 + 4[(MgCo_3)_4.Mg(OH)_2.5H_2O] + 5Nb_2O_5 \Rightarrow 30La(Mg_{2/3}Nb_{1/3})O_3 + 16CO_2 + 24H_2O \quad (2)$$

Powder-processing was carried out as shown schematically in Fig. 1. The methods of mixing, drying, grinding, firing and sieving of the products were similar to those employed in the preparation of the $MgNb_2O_6$ and $FeNbO_4$ powders in our previous work.[21,22] A McCrone vibro-milling technique was employed in order to combine mixing capability with a significant time-saving (only 30 min instead of 12 h, as required in conventional ball-milling[11]). Various calcination conditions, i.e. temperatures ranging from 1000 to 1400°C and times ranging from 4 to 24 h with constant heating and cooling rates of 10°C min^{-1}, were selected, in order to investigate the formation of lanthanum magnesium niobate.

2.2. Sample characterisation

The reactions taking place during heat treatment were investigated by differential thermal analysis (DTA) (NETZSCH-Gerätebau GmbH Thermal Analysis), using a heating rate of 10°C min^{-1} in the temperature range from 100 to 1400°C. Calcined powders were first examined by X-ray diffraction (XRD; Philips PW1700 diffractometer) using CuK_α radiation, in order to identify the phases formed and therefore derive optimum calcination conditions for the manufacture of LMN powder. The particle size distributions of the samples were determined by laser diffraction techniques (MasterSizer, Malvern, UK). Powder morphologies and grain sizes were directly imaged using scanning electron microscopy (both Camscan and Hitachi-700 FEG SEM). The chemical compositions and structures of the phases formed were elucidated by analytical transmission electron microscopy (Philips CM20 TEM/STEM) operated at 200 keV and fitted with an energy-dispersive X-ray (EDX) analyser with an ultra-thin window. EDX spectra were quantified with the virtual standards peaks supplied with the Oxford Instruments eXL software. Powder samples were dispersed in solvent and deposited by pipette on to 3 mm holey carbon grids for observation by TEM. In addition, attempts were made to evaluate the crystal structures of the observed compositions/phases by correlating the XRD and TEM diffraction data.

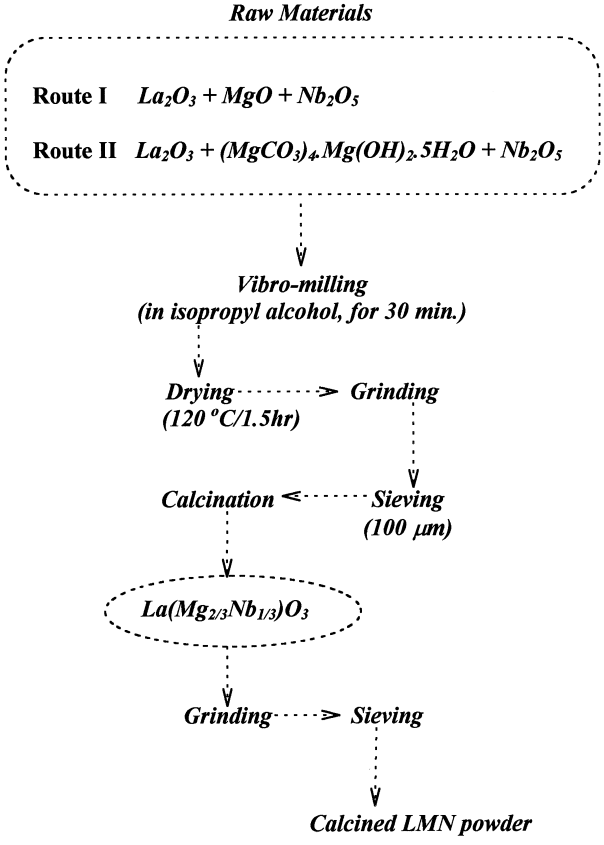

Fig. 1. Preparation route for the $La(Mg_{2/3}Nb_{1/3})O_3$ powder.

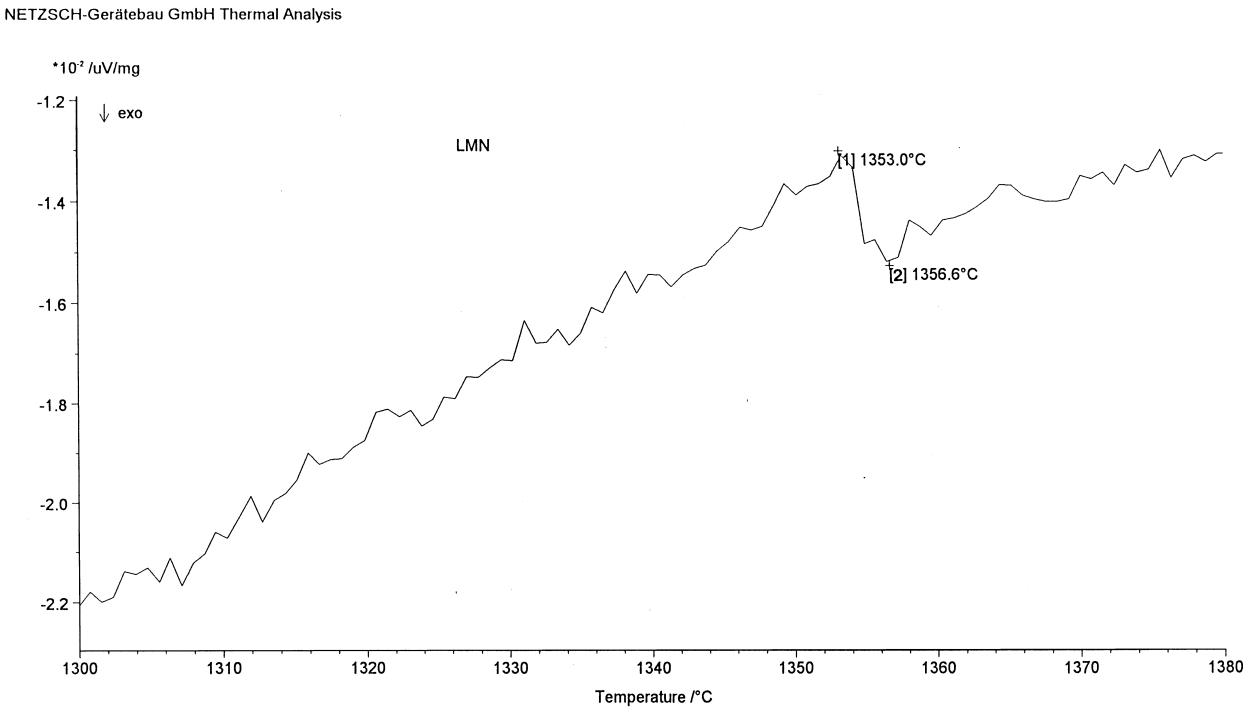

Fig. 2. A DTA curve for the $La(Mg_{2/3}Nb_{1/3})O_3$ powder.

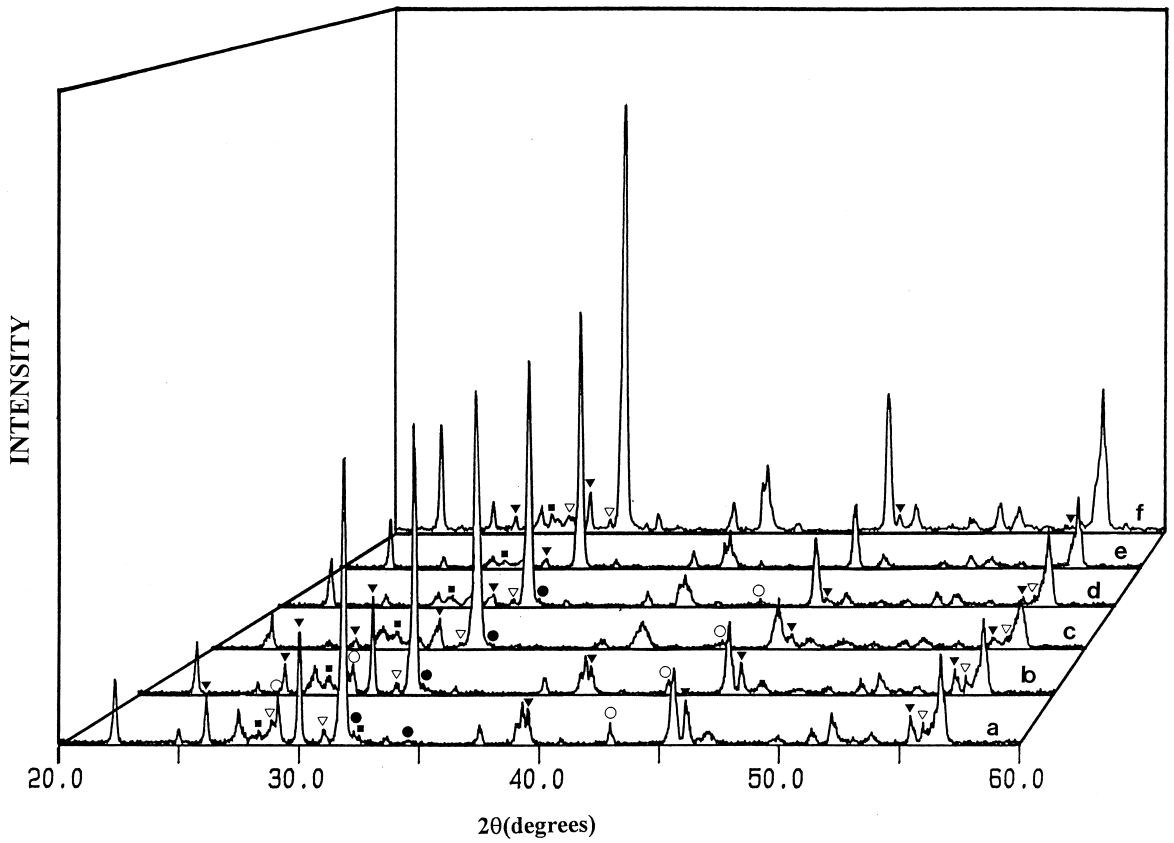

Fig. 3. Powder XRD patterns of the calcined $La(Mg_{2/3}Nb_{1/3})O_3$ (route I) at calcination temperatures (a) 1000°C, (b) 1050°C, (c) 1100°C, (d) 1200°C, (e) 1300°C and (f) 1400°C with constant dwell time for 4 h.

3. Results and discussion

3.1. Identification of the optimum calcination temperature for LMN

A DTA curve obtained for a powder mixed in the stoichiometric proportions of $La(Mg_{2/3}Nb_{1/3})O_3$ is shown in Fig. 2, where an exothermic process is observed in the approximate range from 1353 to 1356°C, these temperatures having been obtained from the calibration of the sample thermocouple. These data, together with those in literature,[9,13,18,19], were used to define the ranges of temperatures (1000–1400°C) and dwell-time (4–24 h) for the XRD investigation. Calcined LMN powders, employing both MgO (Figs. 3 and 4) and $(MgCO_3)_4.Mg(OH)_2.5H_2O$ (Fig. 5) as magnesium sources during powder preparation, were examined by XRD. The optimum calcination temperature for the formation of a high purity LMN phase was found to be about 1375°C, i.e. slightly higher than the upper temperature in Fig. 2. In general, the strongest reflections apparent in the majority of the XRD patterns could be matched with the XRD pattern of LMN powder reported by other workers,[9] who assumed rhombohedral symmetry. However, attempts to index all the reflections by means of a rhombohedral cell failed, even with doubled axes. Moreover, some of the additional peaks could not be matched with the known peaks of likely minor phases. Thus the decision was taken to investigate the structure of the LMN phase by neutron powder diffraction followed by Rietveld refinement. This work, which is reported separately,[23] indicated that LMN has a *monoclinic* perovskite structure, in space group $P2_1/n$ with cell parameters $a = 796.55(9)$ pm, $b = 794.83(5)$ pm, $c = 797.35(8)$ pm, $\beta = 90.534(4)°$ (Fig. 6). By employing this monoclinic symmetry, the presence of the major phase of LMN as well as the minor phases could be determined from the XRD patterns given in Figs. 3–5. Depending on the calcination conditions, at least five minor phases were identified, i.e. $LaNbO_4$ (▽), La_3NbO_7 (■), La_2O_3 (▼), MgO (○), and $Mg_4Nb_2O_9$ (●). The additional reflections of these minor phases can be correlated with JCPDS file nos. 22-1125, 26-822, 5-602, 30-794 and 33-875, respectively. The $LaNbO_4$ phase has a fergusonite-type structure with a primitive monoclinic unit cell

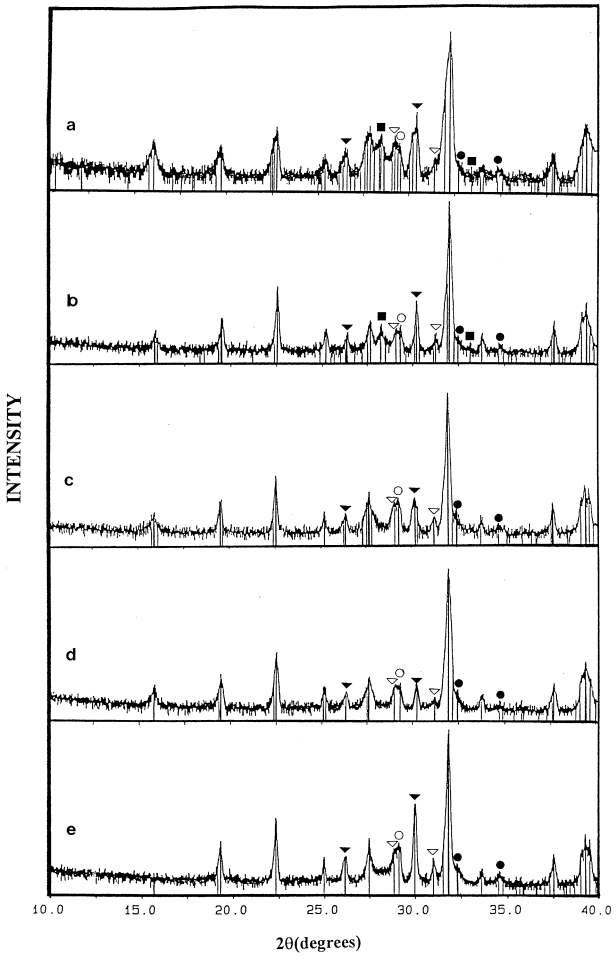

Fig. 4. Powder XRD patterns of the calcined $La(Mg_{2/3}Nb_{1/3})O_3$ (route I) at calcination conditions (a) 1325°C for 4 h, (b) 1350°C for 4 h, (c) 1375°C for 4 h, (d) 1375°C for 8 h and (e) 1000°C for 24 h.

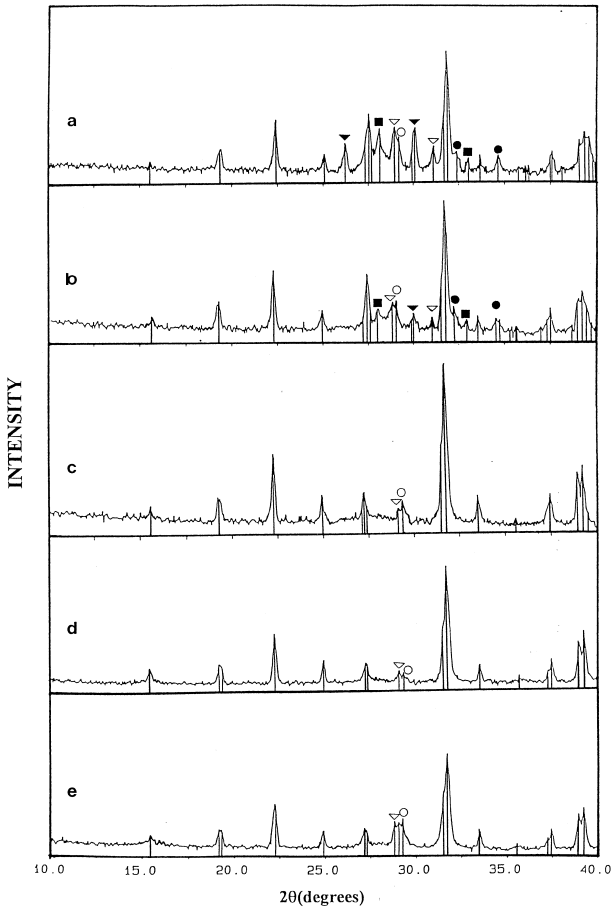

Fig. 5. Powder XRD patterns of the calcined $La(Mg_{2/3}Nb_{1/3})O_3$ (route II) at calcination conditions (a) 1325°C for 4 h, (b) 1350°C for 4 h, (c) 1375°C for 4 h, (d) 1375°C for 8 h and (e) 1000°C for 24 h.

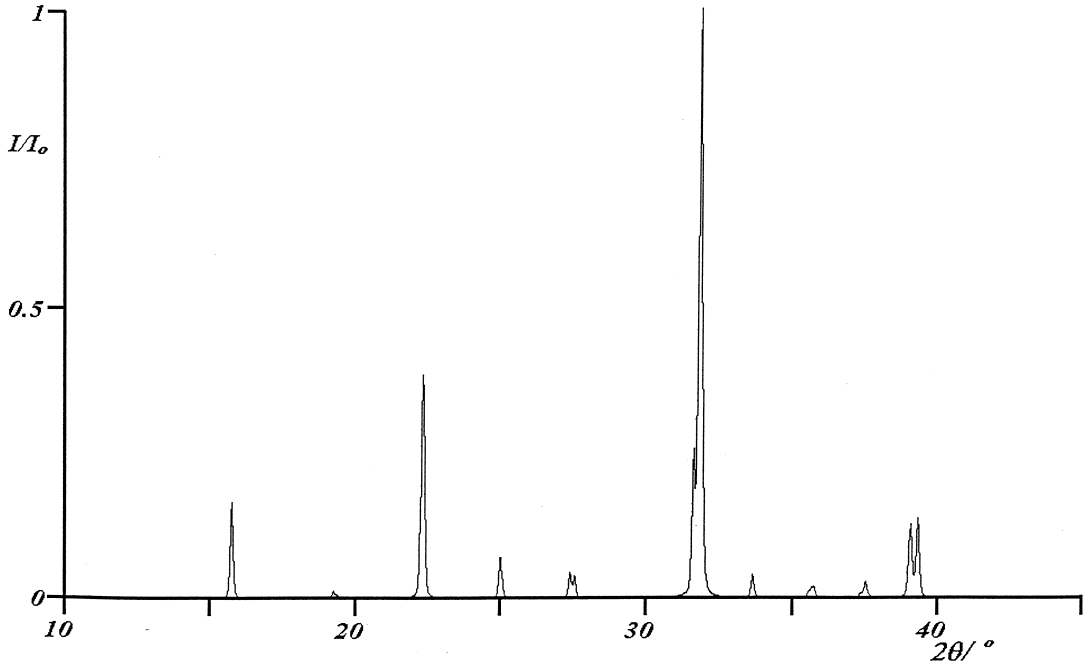

Fig. 6. Predicted XRD pattern of the monoclinic $P2_1/n$ phase of $La(Mg_{2/3}Nb_{1/3})O_3$,[25] generated from atomic coordinated in the accompanying NPD refinement,[23] employing Voigt instrumental peak shapes.

($a=5.57$ Å, $b=11.52$ Å, $c=5.21$ Å and $\beta=94.05°$), space group $I2/c$. La_3NbO_7, by comparison, has an orthorhombic unit cell ($a=7.62$ Å, $b=7.76$ Å and $c=11.15$ Å). Precursor La_2O_3 has a hexagonal unit cell ($a=3.9373$ Å and $c=6.1299$ Å) in space group $P\bar{3}m1$ (No. 164), whereas cubic symmetry ($a=8.12$ Å) is associated with the MgO precursor. The $Mg_4Nb_2O_9$ phase has a corundum-type (α-Al_2O_3) structure with a hexagonal unit cell ($a=5.16$ Å and $c=14.02$ Å), space group $P\bar{3}c1$ (No. 165). No unreacted Nb_2O_5 was observed, nor was there any indication of the columbite-like phase of $MgNb_2O_6$ being present.

The relative amounts of the two majority phases, i.e. perovskite-like LMN and La_2O_3, which are present in each calcined powder, may, in principle, be calculated from the intensities of the most intense X-ray reflections:

Table 1
Phase analysis for calcined LMN powders[a,b]

Route	Calcination conditions		Qualitative concentrations of phases	
	Temperature (°C)	Time (h)	LMN (wt.%)	La_2O_3 (wt.%)
I	1325	4	68.1	31.9
I	1350	4	72.7	27.3
I	1375	4	90.7	9.3
I	1375	8	95.8	4.2
I	1000	24	74.0	26.0
II	1325	4	91.9	8.1
II	1350	4	96.8	3.2
II	1375	4	100.0	0.0
II	1375	8	100.0	0.0
II	1000	24	100.0	0.0

[a] The estimated precision of the concentrations for the two phases is ±0.1%.

[b] The concentration of La_2O_3 phase was calculated as an indicator of the purity of the LMN phase for varying calcination conditions. Concentrations of $LaNBO_4$ and MgO phase were found to be small and relatively constant for all calcination conditions.

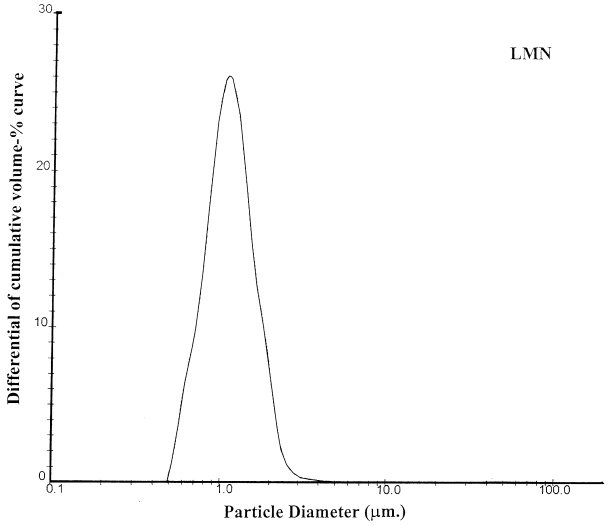

Fig. 7. The particle size distribution curve of the calcined $La(Mg_{2/3}Nb_{1/3})O_3$ powder.

$$\text{wt.\% perovskite phase} = 100 \times \left[\frac{I(LMN)}{I(LMN) + I(La_2O_3)}\right] \quad (3)$$

This equation is analogous to the well known equation[24] widely employed in connection with the fabrication of complex perovskite materials. It should be seen as a first approximation, since its applicability requires comparable maximum intensities of the peaks of perovskite and minor phases. Here $I(LMN)$ and $I(La_2O_3)$ refer to the intensities of the {022} LMN and {101} La_2O_3 peaks, these being the most intense reflections in the XRD patterns of these two phases. For the purpose of estimating the concentrations of the phases present, Eq. (3) has been applied to the powder XRD patterns obtained, as given in Table 1.

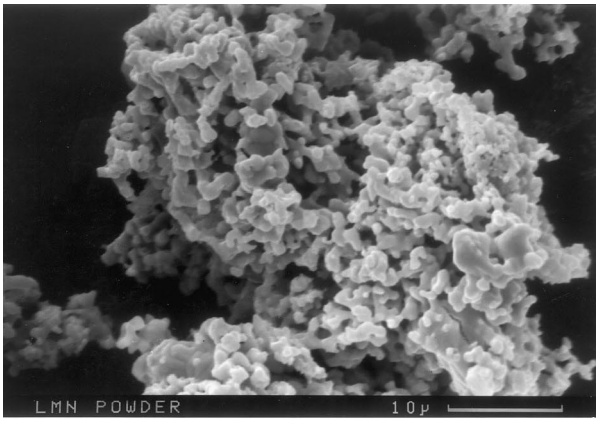

(a)

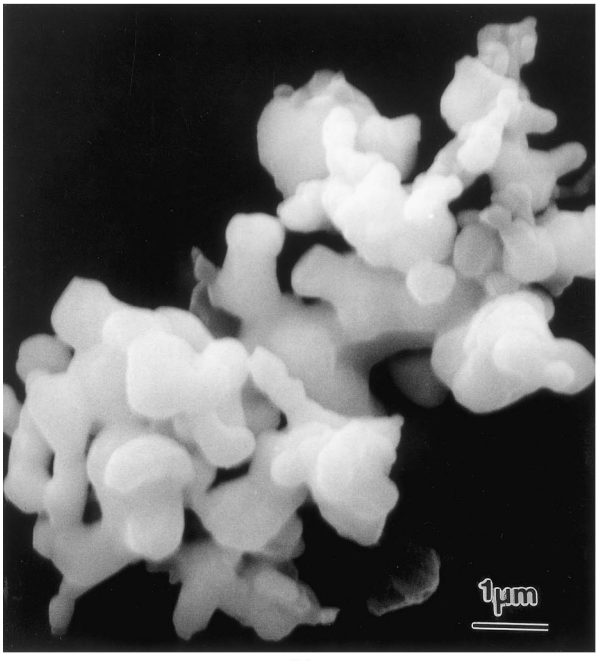

(b)

Fig. 8. SEM micrographs of the calcined $La(Mg_{2/3}Nb_{1/3})O_3$ powder.

This study shows that a solid state, mixed oxide synthetic route for the preparation of LMN leads to inhomogeneous powders. Poor reactivity of the magnesium and lanthanum precursors seems to be a major factor, since relatively high amounts of both unreacted MgO (○) and La_2O_3 (▼) phases were found, together with some minor phases of $LaNbO_4$ (▽), La_3NbO_7 (■), and $Mg_4Nb_2O_9$ (●), particularly at low calcination temperatures. This rationalisation correlates with the findings at high temperatures and long heat treatments, where the amounts of both unreacted precursors and minor phases gradually decrease. Moreover, it is interesting to note that the use of magnesium carbonate hydroxide pentahydrate as a magnesium source (route II) together with the vibro-milling technique can effectively enhance the

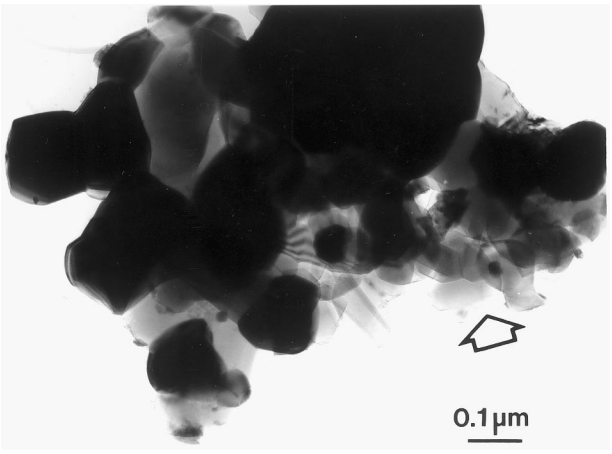

Fig. 9. TEM micrograph of the $La(Mg_{2/3}Nb_{1/3})O_3$ particles; arrows indicate MgO-rich areas in LMN parent phase.

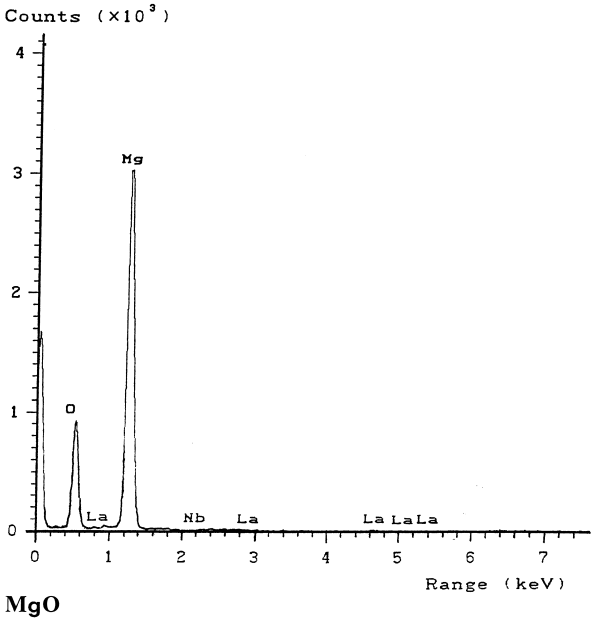

Fig. 10. EDX analysis of the MgO-rich regions.

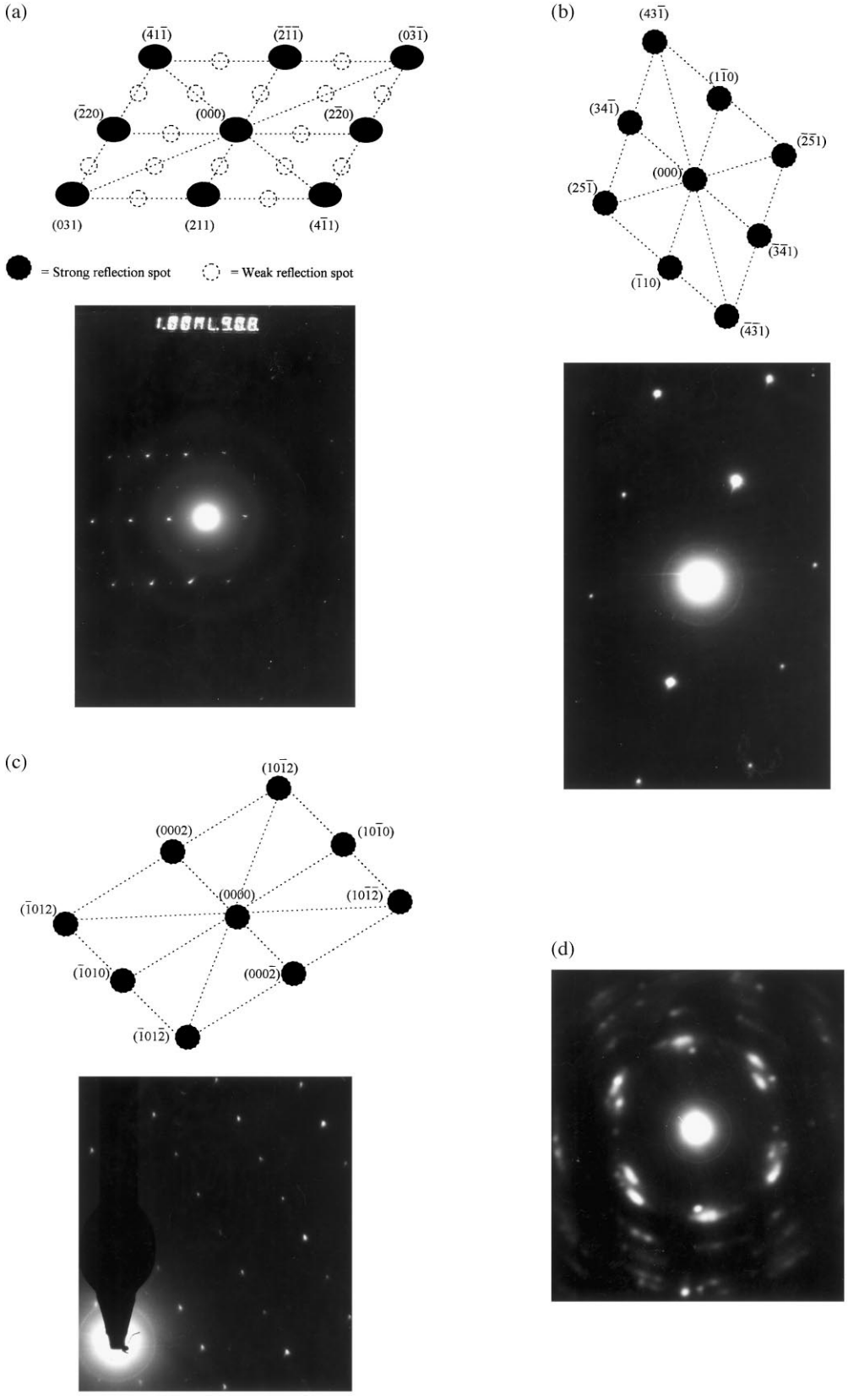

Fig. 11. SAED patterns of the major phase of (a) rhombohedral $La(Mg_{2/3}Nb_{1/3})O_3$ ([113] zone axes) and minor phases of (b) monoclinic $LaNbO_4$ phase ([117] zone axis), (c) hexagonal $Mg_4Nb_2O_9$ phase ([01$\bar{1}$0] zone axis) and (d) hexagonal La_2O_3 phase.

yield of the LMN phase (Fig. 5). As the firing temperature is raised, more of the LMN phase is formed in the products, with corresponding decreases in the concentrations of all minor phases (Figs. 3–5). At a calcination temperature of about 1375 °C and longer heat treatment conditions [Fig. 5(c–e)], no minor phases of La_3NbO_7, La_2O_3 and $Mg_4Nb_2O_9$ could be found within the detection limits of XRD. However, the formation of $LaNbO_4$ (▽) and unreacted MgO (○) could not be completely eliminated. In earlier work[9] long heat treatments at 1000°C for 24 h were proposed for the formation of LMN by a conventional mixed oxide synthetic route, although no details on phase formation were provided. In the present study, an attempt was also made to calcine LMN powders under the conditions advocated by Lin and Wu[9] [Figs. 4(e) and 5(e)]. In this connection, it was found that some XRD reflections of two minor phases $LaNbO_4$ (▽) and MgO (○) could still be detected alongside the majority LMN phase. The sequence of reactions during calcination may be inferred from the XRD investigation as follows:

- for calcination conditions between 1000 and 1350°C for 4 h (both routes I and II)

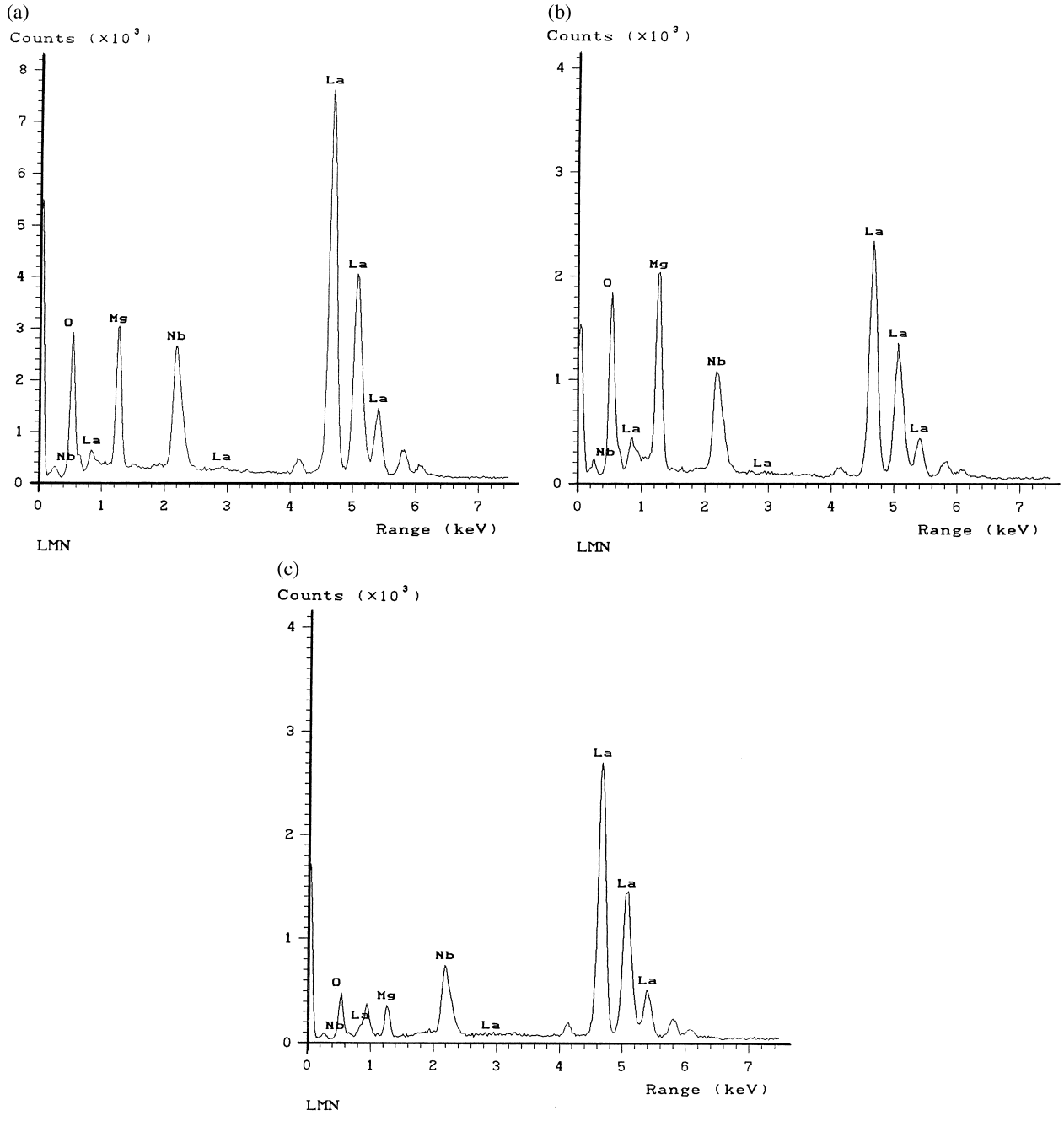

Fig. 12. EDX analysis of the major phase $La(Mg_{2/3}Nb_{1/3})O_3$ indicating the variation of Mg/Nb ratio.

La_2O_3 + [MgO or $(MgCO_3)_4.Mg(OH)_2.5H_2O$] + $Nb_2O_5 \Rightarrow La(Mg_{2/3}Nb_{1/3})O_3$, $LaNbO_4$, La_3NbO_7, La_2O_3, MgO and $Mg_4Nb_2O_9$;

- for calcination conditions 1375°C (and 1400°C for route I) for 4, 8 h and 1000°C for 24 h
  - Route I: $La_2O_3 + MgO + Nb_2O_5 \Rightarrow La(Mg_{2/3}Nb_{1/3})O_3$, $LaNbO_4$, La_2O_3, MgO and $Mg_4Nb_2O_9$;
  - Route II: $La_2O_3 + (MgCO_3)_4.Mg(OH)_2.5H_2O + Nb_2O_5 \Rightarrow La(Mg_{2/3}Nb_{1/3})O_3$, $LaNbO_4$ and MgO

It may be concluded that, over a wide range of calcination conditions, single phase perovskite-like LMN cannot be straightforwardly formed via a solid state mixed oxide synthetic route. The mechanisms behind the formation of LMN perovskite are therefore somewhat complex and unclear. For the purposes of the present study, LMN powders synthesised by route II and calcined at 1375°C for 4 h were selected for further investigation.

3.2. Particle size analysis

Fig. 7 shows the particle size distribution of $La(Mg_{2/3}Nb_{1/3})O_3$ powder after calcination at 1375°C for 4 h, indicating a uniform frequency distribution curve with an appreciable size fraction at about 1.2 μm within the range 0.5 to 5.0 μm.

3.3. Electron microscopy analysis

SEM micrographs of the calcined $La(Mg_{2/3}Nb_{1/3})O_3$ powder (1375°C for 4 h) are given in Figs. 8(a) and (b). The particles are agglomerated and basically irregular in shape, with a substantial variation in particle size. However, some spherical particles could be found at high magnification, ranging in diameter from 0.5–5.5 μm, in good agreement with the particle size distribution determined previously (Fig. 7).

A bright field TEM image of discrete particles of the calcined $La(Mg_{2/3}Nb_{1/3})O_3$ powder is shown in Fig. 9, indicating the particle sizes and shapes at higher magnification. The observed morphology reveals the considerable variation in sizes and shapes of the particles. The particle diameter was found to be about 0.5–1.5 μm in these TEM micrographs. A combination of TEM and EDX techniques has demonstrated that an MgO-rich phase (arrowed) exists neighbouring the LMN parent phase (thicker area; blocky crystals), as shown in Figs. 9 and 10. By employing a combination of both selected area electron diffraction (SAED) and crystallographic analysis, the major phase of monoclinic LMN and minor phases of monoclinic $LaNbO_4$ and hexagonal $Mg_4Nb_2O_9$ were identified [Fig. 11(a)–(c)], in good agreement with the XRD results. In general, EDX analysis using a 20 nm probe from a large number of particles of the calcined powder confirmed the parent composition to be $La(Mg_{2/3}Nb_{1/3})O_3$ [Figs. 12(a)–(c)]. However, a variation in the Mg/Nb ratio was clearly apparent. Minor phases of $LaNbO_4$ and $Mg_4Nb_2O_9$ were also confirmed by this technique, as illustrated in Figs. 13-14 and Table 2. Moreover, limited evidence for the presence of the unreacted starting precursors La_2O_3 [Fig. 11(d) — the ring patterns indicating the polycrystalline nature and hence fine scale of this phase] and MgO (Fig. 10) was also found in the TEM-EDX investigation, even though these could not be detected by XRD.

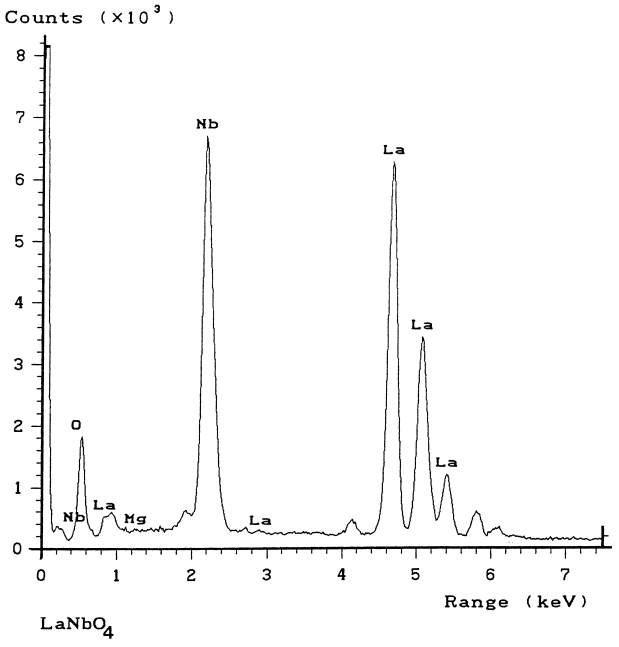

Fig. 13. EDX analysis of the minor phase $LaNbO_4$.

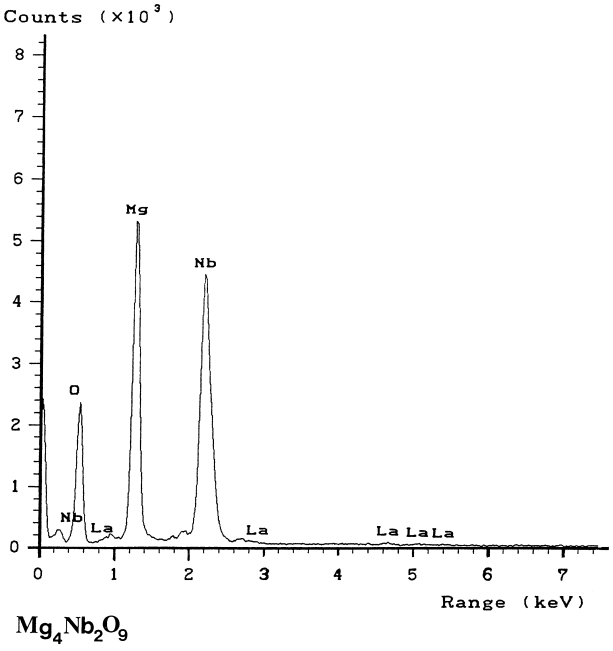

Fig. 14. EDX analysis of the minor phase $Mg_4Nb_2O_9$.

Table 2
Chemical compositions of calcined LMN powders (1375°C for 4 h route II) from TEM-EDX analysis

Composition (at.%)			Possible phases
La (L)	Mg (L)	Nb (K)	
39.9	43.6	16.4	$La(Mg_{2/3}Nb_{1/3})O_3$
56.3	25.5	18.2	$La(Mg_{2/3}Nb_{1/3})O_3$
40.3	32.9	26.8	$La(Mg_{2/3}Nb_{1/3})O_3$
48.3	50.9	–	$LaNbO_4$
–	71.2	28.6	$Mg_4Nb_2O_9$
100.0	–	–	La_2O_3
–	100.0	–	MgO

4. Conclusion

The complex perovskite-type compound $La(Mg_{2/3}Nb_{1/3})O_3$ has been prepared by a solid state mixed oxide synthetic route. The preparative method involved the use of laboratory-grade precursors, low milling and drying times of powders, together with moderately low calcination times. A combination of X-ray and electron diffraction studies has demonstrated inhomogeneity in LMN powders with a MgO-rich phase distributed over the majority phase and fluctuations in the Mg/Nb concentration ratio within the LMN phase. Minor phases were identified as La_2O_3, $LaNbO_4$, La_3NbO_7, MgO and $Mg_4Nb_2O_9$, with their concentrations decreasing at higher calcination temperatures.

Acknowledgements

One of the authors (S.A.) wishes to acknowledge the DPST project and the Thai Government for financial support during his study. Thanks are also due to Mr. J. Harrington for his valuable assistance with SEM, to Mr. D. Wright for carrying out XRD, and to Mrs. S. Andrews for operating the DTA apparatus at WBB Technology.

References

1. Galasso, F. S., *Structure and Properties of Inorganic Solids*. Pergamon Press, Oxford, 1970 172–204.
2. Anon. *Landolt-Börnstein, New Series III*, Vol. 16a, Springer-Verlag, Berlin, 1981.
3. Lines, M. E. and Glass, A. M., *Principles and Applications of Ferroelectrics and Related Materials*. Clarendon Press, Oxford, 1977.
4. Shrout, T. R. and Halliyal, A., Preparation of Lead-Based Ferroelectric Relaxors for Capacitors. *Am. Ceram. Soc. Bull.*, 1987, **66**, 704–711.
5. Thomas, N. W., Crystal structure-physical property relationships in perovskites. *Acta Cryst.*, 1989, **B45**, 337–344.
6. Miyazawa, Y., Uchino, K. and Nomura, S., Bulk photovoltaic effect in the $PbTiO_3$–$La(Zn_{2/3}Nb_{1/3})O_3$ solid solution ceramics. *Ferroelectrics Lett.*, 1983, **44**, 341–347.
7. Chen, J., Chan, H. M. and Harmer, M. P., Ordering structure and dielectric properties of undoped and La/Na-doped $Pb(Mg_{1/3}Nb_{2/3})O_3$. *J. Am. Ceram. Soc.*, 1989, **72**, 593–598.
8. Lin, L. J. and Wu, T. B., Ordering behaviour of lead magnesium niobate ceramics with A-site substitution. *J. Am. Ceram. Soc.*, 1990, **73**, 1253–1256.
9. Lin, L. J. and Wu, T. B., Structure evolution from $Pb(Mg_{1/3}Nb_{2/3})O_3$ to $La(Mg_{1/3}Nb_{2/3})O_3$. *J. Am. Ceram. Soc.*, 1991, **74**, 1360–1363.
10. Kim, N., Huebner, W., Jang, S. J. and Shrout, T. R., Dielectric and piezoelectric properties of lanthanum-modified lead magnesium niobate–lead titanate ceramics. *Ferroelectrics*, 1989, **93**, 341–349.
11. Pan, X., Kaplan, W. D., Rhle, M. and Newnham, R. E., Quantitative comparison of transmission electron microscopy techniques for the study of localized ordering on a nanoscale. *J. Am. Ceram. Soc.*, 1998, **81**, 597–605.
12. Fang, F., Gui, H. and Zhang, X., A-site cation ordering and the glassy polarization behaviour of lanthanum-modified lead zirconate titanate. *Ferroelectrics*, 1996, **175**, 233–239.
13. Wu, T. B., Shyu, M., Chung, C. C. and Lee, H. Y., Phase transition and ferroelectric characteristics of $Pb[(Mg_{1/3}Nb_{2/3})_{1-x}Ti_x]O_3$ ceramics modified with $La(Mg_{1/3}Nb_{2/3})O_3$. *J. Am. Ceram. Soc.*, 1995, **78**, 2168–2174.
14. Setter, N. and Cross, L. E., The contribution of structural disorder to diffuse phase transitions in ferroelectrics. *J. Mater. Sci.*, 1980, **15**, 2478–2482.
15. Randall, C. A., Bhalla, A. S., Shrout, T. R. and Cross, L. E., Classification and consequences of complex lead perovskite ferroelectrics with regard to B-site cation order. *J. Mater. Res.*, 1990, **5**, 829–834.
16. Chai, L. and Davies, P. K., Effect of M^{4+} (Ce, Sn, Ti) B-site substitutions on the cation ordering in $Ba(Mg_{1/3}Ta_{2/3})O_3$. *Mater. Res. Bull*, 1998, **33**, 1283–1292.
17. Nagai, T., Sugiyama, M., Sando, M. and Niihara, K., Structural changes in $Ba(Sr_{1/3}Ta_{2/3})O_3$-type perovskite compounds upon tilting of oxygen octahedra. *Jpn. J. Appl. Phys.*, 1997, **36**, (1/3A) 1146–1153.
18. Tavernor, A. W., *Modelling of Relaxor Ferroelectrics*. PhD thesis, University of Leeds, UK, 1992
19. Tavernor, A. W. and Thomas, N. W., Dielectric properties of A and B site substituted lead magnesium niobate. In *British Ceramic Proceedings*, Vol. 52, ed. W. E. Lee and A. Bell. The Institute of Materials, London, 1994, pp. 167–184.
20. Akbas, M. A. and Davies, P. K., Structure and dielectric properties of the $Ba(Mg_{1/3}Nb_{2/3})O_3$–$La(Mg_{2/3}Nb_{1/3})O_3$ system. *J. Am. Ceram. Soc.*, 1998, **81**, 2205–2208.
21. Ananta, S., Brydson, R. and Thomas, N. W., Synthesis, formation and characterisation of $MgNb_2O_6$ powder in a columbite-like phase. *J. Eur. Ceram. Soc.*, 1999, **19**(3), 355–362.
22. Ananta, S., Brydson, R. and Thomas, N. W., Synthesis, formation and characterisation of $FeNbO_4$ powders. *J. Eur. Ceram. Soc.*, 1999, **19**(4), 489–496.
23. Ivanov, S. A., Thomas, N. W., Ananta, S., Tellgren, R. and Rundlof, H., The perovskite system $La(Mg_{2/3}Nb_{1/3})O_3$ II A neutron powder diffraction study. *J. Eur. Ceram. Soc.*, 2000, **20**, 2325–2329.
24. Swartz, S. L. and Shrout, T. R., Fabrication of Perovskite lead magnesium niobate. *Mat. Res. Bull.*, 1982, **17**, 1245–1250.
25. Thomas, N. W., *Xrps Software package*. WBB Proprietary Software, 1998.